Isothermal crystallization of end-linked poly(tetrahydrofuran) networks

Mitsuhiro Shibayama*, Hiroshi Takahashi, Hideki Yamaguchi, Shinichi Sakurai and Shunji Nomura

Department of Polymer Science and Engineering, Kyoto Institute of Technology, Matsugasaki, Sakyo-ku, Kyoto 606, Japan

(Received 20 September 1993; revised 9 November 1993)

End-linked networks of poly(tetrahydrofuran) (PTHF) having a narrow molecular weight distribution were prepared by living cationic polymerization of PTHF followed by a crosslink reaction with pentaerythritol tetrakis(3-mercaptopropionate). It was found that the PTHF network was capable of crystallization even in the presence of crosslinks. The rate of isothermal crystallization at 20°C was of the order of days. The crystallization kinetics of the networks in a film form at 20°C was studied by monitoring the ageing time dependence of the mechanical and thermal properties, and infra-red absorption (i.r.) spectra. The mechanical behaviour was typical of that of elastomers in the induction and/or early stage of crystallization ($\sim$300 min). However, it changed gradually to that of semicrystalline polymers at the late stage ($\sim$5670 min). The Avrami exponent was estimated by two methods, i.e. time evolution of the characteristic i.r. absorption band (i.r. method) and of the enthalpy of fusion (differential scanning calorimetry) (d.s.c.) method. The exponents were 2.2 by the i.r. method and 2.4 by the d.s.c. method. Morphological studies on the aged films revealed the presence of spherulites of the order of 50 to 100 μm, which were much larger than those for prepolymers (25 to 50 μm). The effects of crosslinks on the crystallization kinetics and morphology as well as on the mechanical properties are discussed.

(Keywords: poly(tetrahydrofuran); crystallization; network)

INTRODUCTION

Recent developments of tailor-made polymer networks by end-linking of well fractionated prepolymers enabled a direct comparison between experimental results and theoretical predictions on elastomers[1]. These networks have been used as a model network, having a fairly narrow molecular weight distribution between crosslinks and negligible amounts of architectural defects, such as dangling chains and loops. These well defined polymer networks were employed to examine the statistical theory of elasticity, such as the affine network model[2], phantom network model[3], constraint junction model[4] and slip-link model[5]. Mark and Sullivan studied the elastic modulus and the equilibrium degree of swelling for end-linked polydimethylsiloxane (PDMS) and reported that the mechanical properties and swelling behaviours were well predicted by the Mooney–Rivlin equation and by the Flory–Rehner theory, respectively[6]. It then became clear that there was a significant difference in the mechanical properties between an end-linked model network and a randomly crosslinked network[7]. This finding triggered a series of studies of bimodal polymer networks so as to clarify the effects of polydispersity of the molecular weight between crosslinks on the mechanical and swelling behaviours[1,8,9].

In these studies, fractionated telechelic prepolymers were employed to prepare model networks, of which molecular weight distribution lay around 1.2 to 2.0. Compared with these networks, more suitable model networks were synthesized by cationic living polymerization of poly(tetrahydrofuran) (PTHF) having allyl groups at the both ends followed by a coupling with four-functional crosslinking reagent by Jong and Stein[10]. They studied the mechanical properties of a series of well defined networks of PTHF and found that the estimated molecular weight between crosslinks, M_c, was about a half that of prepolymers. They concluded that this was due to the presence of physical crosslinks formed by trapped entanglements. Hanyu and Stein studied the molecular orientation of bimodal networks composed of long and short PTHF chains[11]. They observed that the short and long chains were deformed with different elongation ratios by stretching and concluded the presence of a non-affine deformation mechanism. Since PTHF is capable of crystallization at room temperature, these studies on PTHF networks were conducted at a temperature above the melting temperature of PTHF, i.e. at 40°C.

In our previous paper, a characterization of PTHF networks prepared by the same method employed by Jong and Stein[10] was reported[12]. The PTHF prepolymers having allyl end groups were well characterized by titration, ^{1}H n.m.r., gel-permeation chromatography and vapour pressure osmometry. The number-average molecular weight, the polydispersity index and the average functionality of the bulk-polymerized PTHF at 0°C for 40 min were 5510, 1.15 and 1.90, respectively. These values for the polydispersity and the functionality seem to be relevant for molecular characterization of the rubber

*To whom correspondence should be addressed

0032-3861/94/14/2944–08

elasticity. The PTHF prepolymers were then crosslinked with pentaerythritol tetrakis(3-mercaptopropionate) and thus a PTHF model network was prepared. It was found that the PTHF network was capable of crystallization at room temperature with a rate much slower than the corresponding PTHF prepolymer. A preliminary experiment on the crystallization of the PTHF network indicated the importance of the crystal characterization as a function of the ageing time and the thermal hysteresis so as to understand the mechanical and thermal properties of the PTHF network[12].

In this paper, we study the crystallization kinetics of the PTHF networks by mechanical measurements, infrared absorption spectroscopy (i.r.) and differential scanning calorimetry (d.s.c.) and discuss the effect of the crosslinks on the crystallization kinetics. First, we review the preparation and characterization of the PTHF network. Then the kinetics of isothermal crystallization of PTHF networks at 20°C after annealing at a temperature above the melting temperature of prepolymer ($T_m \cong 38$°C) will be discussed based on the results of the stress-elongation behaviour, i.r. and d.s.c. Morphological studies by optical microscopy and light scattering will support the proposed kinetics of PTHF network crystallization.

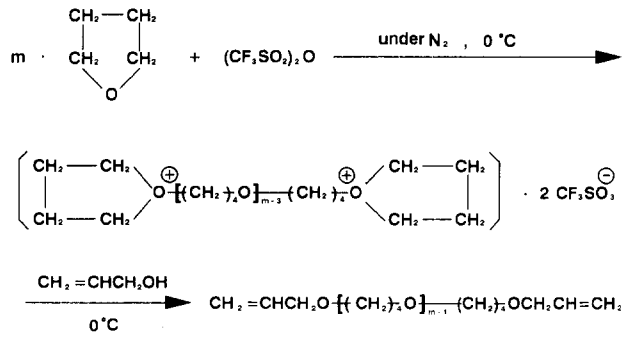

Figure 1 Scheme for the synthesis of the allyl-terminated PTHF

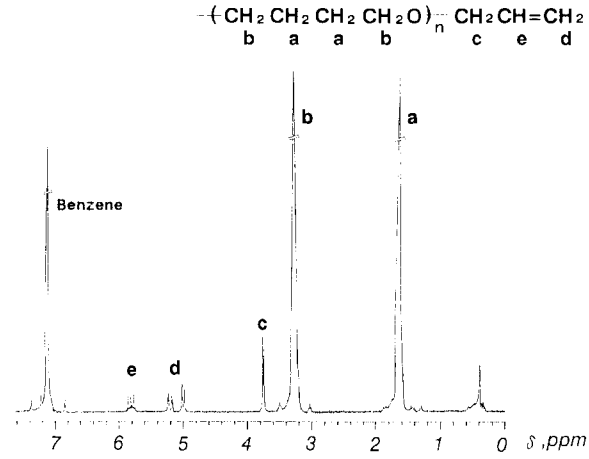

Figure 2 ^{1}H n.m.r. spectrum of the allyl-terminated PTHF

EXPERIMENTAL

Synthesis of prepolymer

Tetrahydrofuran (THF) of guaranteed reagent grade was distilled at least three times over lithium aluminium hydride. Trifluoromethanesulfonic acid anhydride was prepared according to the method reported by Burdon *et al.*[13] and purified by distillation in the presence of diphosphorus pentaoxide just before use. Allyl alcohol and triethylamine of reagent grade were used as received.

The synthetic procedure for the PTHF prepolymer, which is shown in *Figure 1*, is a cationic living polymerization of THF with trifluoromethanesulfonic acid anhydride. The details of the synthesis are as follows: 2.7 ml of trifluoromethanesulfonic acid anhydride was added to 200 ml of THF to initiate polymerization. Then the mixture was stirred with a magnetic stirrer at 0°C for 25 min. In order to terminate the polymerization, 150 ml of allyl alcohol was added to the living polymer solution. The termination reaction was carried out for 30 min at 0°C. Next, 17 ml triethylamine was added into the reaction mixture to neutralize the reaction mixture. Afterwards, the reaction mixture was condensed by a rotary evaporator. The remaining mixture was dissolved in diethyl ether and then washed with water. After evaporation of diethyl ether, the polymer was dissolved in benzene and freeze-dried. Thus telechelic PTHF prepolymers having allyl end groups were synthesized by the addition of allyl alcohol as the terminator to the dicationic PTHF ends.

Characterization of prepolymer

The number-average molecular weight of the prepolymer, M_n, was measured at 37°C with a vapour pressure osmometer (VPO, Knauer). Benzene was used as a solvent. M_n was determined to be 5190. The molecular weight distribution was measured to be 1.17 by a Trirotar II GPC (Jasco). The functionality of the allyl groups per chain was determined with a 300 MHz QE-300 NMR Spectrometer (General Electric). A typical n.m.r. spectrum of PTHF prepolymer in deuterated benzene is shown in *Figure 2*. As shown in the figure, peaks a and b are assigned to the PTHF protons and peaks c–e to allyl protons. The functionality was determined to be 1.94 by taking the ratio of the integrated peaks of the PTHF protons and allyl protons.

Preparation of end-linked PTHF network

The end-linked PTHF network was prepared by crosslinking the PTHF prepolymer with pentaerythritol tetrakis(3-mercaptopropionate) [$C(CH_2OCOCH_2CH_2SH)_4$]. The crosslinking was introduced by a reaction of –SH group of the crosslinker and $-CH{=}CH_2$ group of the prepolymer. Stoichiometric amounts of the prepolymer and the crosslinker and benzopinacol, the initiator (0.35 wt% of prepolymer and crosslinker), were mixed in toluene. The concentration of this solution was about 8 wt%. The solution was poured into a stainless steel mould and was cast at room temperature. The crosslinking reaction was carried out by keeping the cast film at 88°C under N_2 for 48 h. In order to evaluate the sol fraction of the network film, a part of the film was soaked in toluene. The sol fraction, estimated from the weight of the network before and after extraction, was 0.136.

The PTHF network film, annealed at 60°C for 2 h, was isothermally crystallized in a sealed chamber dipped in a water circulating bath controlled at 20.0 ± 0.1°C.

Stress–elongation measurement

Stress–elongation behaviours of isothermally crystallized PTHF network films were examined with an UTM-II-5H (Orientec) in a temperature-controlled room at 20 ± 1°C. The film strips were 30 mm long, 10 mm wide

and about 100 μm thick. The stretching rate was 20 mm min^{-1}.

Differential scanning calorimetry (d.s.c.)

D.s.c. measurements were conducted using a DSC3100 (MAC Science). The heating rate was 5°C min^{-1}. The samples which were punched out from the network film and crimpled in an aluminium pan were isothermally crystallized in the sealed chamber at 20.0±0.1°C for a given time after annealing at 60°C. Then the sample pans were quickly transferred to the d.s.c. chamber and a thermogram was recorded during the heating process.

Infra-red absorption (i.r.) spectroscopy

PTHF network films of about 60 μm thick, aged in the manner discussed above, were used for i.r. absorption experiments. In the case of the reference sample, the sample was aged at 20°C for a week in a desiccator. I.r. absorption spectra were obtained on a FIRIS 100 Fourier-transform infra-red spectrometer (Fuji Electric). The number of scans and the resolution were 64 and 4 cm^{-1}, respectively.

Light-scattering measurement and optical microscopy

Light-scattering patterns of network and prepolymer films of about 60 μm thick were obtained photographically with a laboratory-made light-scattering apparatus coupled with a 5 mW He–Ne laser. Cross-polarized optical micrographs were taken for aged network and prepolymer films with a Nikon polarized microscope.

RESULTS AND DISCUSSION

Mechanical behaviour

Figure 3 shows the ageing time dependence of the nominal stress–elongation ratio curves. The time in the figure denotes the ageing time, t. For the sample aged for 30 min, the stress increases gradually with elongation up to the elongation ratio, $\alpha=4$. This kind of mechanical behaviour is typical of that for elastomers. For $\alpha>4$, the stress increases rather steeply, indicating the occurrence of the so-called strain-induced crystallization as well as an orientation effect due to non-Gaussian nature of rubber elasticity, e.g. an inverse Langevin chain behaviour. With increasing ageing time, t, the initial slope of the stress–elongation ratio curve increases and the rubbery-type mechanical behaviour changes to that of crystalline polymers. For example, the network film of $t=5670$ min has a distinct yield point and a plateau region up to $\alpha=2.7$, a typical stress–elongation behaviour for crystalline polymers.

Now we evaluate the time evolution of the mechanical properties with respect to the change of the effective molecular weight between crosslinks, M_c, by assuming that crystallites formed in the network films during the isothermal crystallization play as crosslinks and the Mooney–Rivlin equation[14] can be applied. The Mooney–Rivlin equation is given by

$$f^* \equiv \frac{f}{\alpha-\alpha^{-2}} = 2C_1 + 2C_2\alpha^{-1} \qquad (1)$$

where f^* is the reduced stress, f the nominal stress, and α is the elongation ratio. $2C_1$ and $2C_2$ are the Mooney–Rivlin constants. $2C_1$ is related to the molecular weight between crosslinks, M_c, via

$$M_c = \frac{A\rho RT\phi^{2/3}}{2C_1} \qquad (2)$$

where A is the structure factor of the network, ρ the mass density, R the gas constant, T the absolute temperature and ϕ the volume fraction of the polymer. A is given by

$$A = 1 - \frac{2}{f_x} \qquad (3)$$

for a network having the functionality of f_x. *Figure 4* shows the plots of f^* *versus* α^{-1} for sample films having different ageing time. By extrapolating the values of f^* for $\alpha^{-1}>0.3$ to $\alpha^{-1}=0$, $2C_1$ was estimated for each t. We assume here that the functionality, f_x, of the crosslinker is 4, and ϕ is estimated to be 0.864 by taking account of the sol fraction of the as-prepared PTHF network. By substituting these values in equations (3) and (2), M_c was estimated as a function of t, which is shown in *Figure 5*. The data points fall roughly on a straight line having a negative slope. This indicates that the number of crosslinks increases with ageing of the network. It should be noted here that the intercept gives the value of M_c of the film at $t=0$ and the estimated value of 5.2×10^3 is in good accordance with the molecular weight of the prepolymer, $M_n=5190$. It should

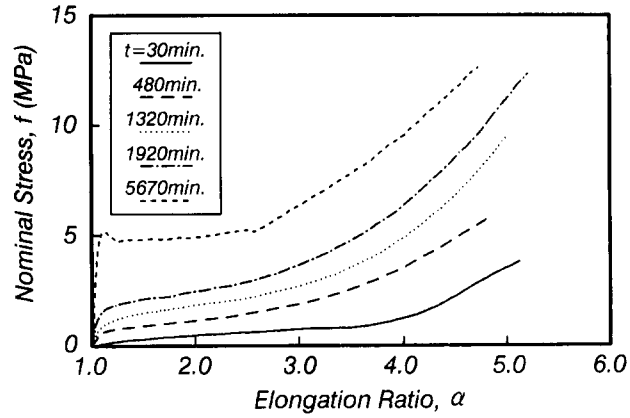

Figure 3 Ageing time dependence of the nominal stress-elongation ratio curves. The time in the figure denotes the ageing time, t

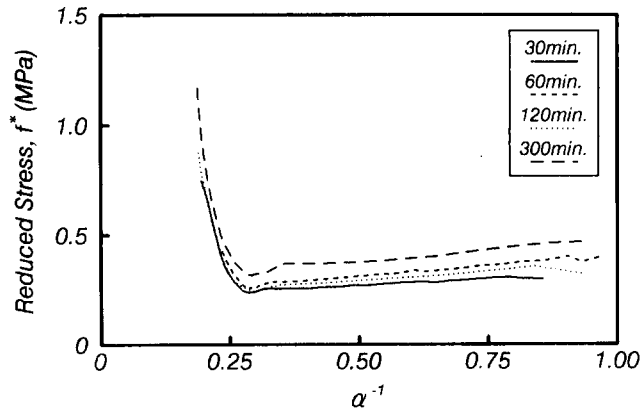

Figure 4 Mooney–Rivlin plots for the end-linked PTHF networks. f^* and α^{-1} are the reduced stress and inverse of the elongation ratio, respectively

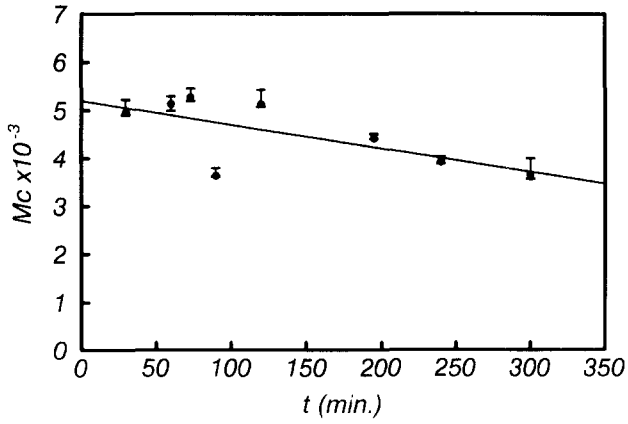

Figure 5 Ageing time dependence of the average molecular weight between crosslinks, M_c

also be noted here that we assume zero-volume crosslinks in the discussion of equation (2). This assumption is incorrect particularly for the case when additional crosslinks are formed via crystallization of PTHF. However, we assume that this effect of the finite volume of crosslinks is negligible for $t < 300$ min.

This assumption does not alter the main conclusion of this study. The number density of the crosslinks ν, for a network having a functionality of 4, is estimated by

$$\nu(t) = \frac{mN_A}{2V}\frac{1}{M_c} \tag{4}$$

where m, V and N_A are the molecular weight and the volume of the monomeric unit and Avogadro's number. Since M_c is a function of t in this study, ν is shown here explicitly as a function of t. According to the variation of M_c, $\nu(t)$ increases almost linearly with t, from $\nu(0) = 5.67 \times 10^{19}\,\mathrm{cm}^{-3}$ to $\nu(300\,\mathrm{min}) = 8.07 \times 10^{19}\,\mathrm{cm}^{-3}$. $\nu(0)$ is regarded as the initial number density of the crosslinker, i.e. pentaerythritol tetrakis(3-mercaptopropionate). The excess number in $\nu(t)$, increasing with t, indicates the time evolution of physical nuclei consisting of PTHF crystallites. We did not estimate M_c and $\nu(t)$ for $t > 300$ min because the stress–elongation curves deviated from those for elastomers and equation (1) was not applicable.

The time dependence of the mechanical behaviour seen in *Figure 3* and that of M_c in *Figure 5* clearly indicates that an isothermal crystallization of the crosslinked PTHF takes place and the number of effective crosslinks increases during the ageing at 20°C.

Infra-red absorption

Infra-red absorption spectroscopy is a sensitive tool for checking the presence of crystalline structures in a polymer film. *Figure 6* shows the infra-red absorption spectra for films of before ($t = 0$) and after ($t = \infty$) crystallization. When $t = \infty$ the crystallization is complete and the film is in an equilibrium state, which is obtained by ageing for a week at 20°C. By comparing the two spectra, the following facts are disclosed: (1) The symmetric stretching band of COC, ν_s(COC) at 997 cm^{-1} and the CC stretching band, ν(CC), at 1011 cm^{-1} do not exist for the film of $t = 0$ but exist for $t = \infty$. (2) The four absorption bands in the region 1420–1500 cm^{-1}, assigned to the in-plane bending of CH_2, $\delta(CH_2)$, change their peak positions as well as their absorbance. (3) Differences in the spectra are also found in the CH_2 out-of-plane wagging vibration at 1371 and 1240 cm^{-1}, $\omega(CH_2)$, and in the CH_2 out-of-plane twisting vibration, $\tau(CH_2)$ at 1210 cm^{-1}. The carbonyl absorption band of C=O stretching vibration, ν(C=O), due to the presence of crosslinker is also observed at 1743 cm^{-1}. Since this absorption band is not affected by the crystallization of PTHF, we employ this as an internal standard for the infra-red absorption analysis.

Figure 7 shows the time evolution of absorption spectra, $\delta(CH_2)$, in the region 1410–1530 cm^{-1}. Although the absorption band at 997 cm^{-1} shows a more distinct change with time, the absorbance was too large to assume the Lambert–Beer law. Thus we did not employ this band for the analysis. We focus on the absorption at 1447 cm^{-1} which decreases gradually with time. *Figure 8* shows the time evolution of the normalized absorbance at 1447 cm^{-1}. The normalization was conducted with respect to the carbonyl absorption band at 1743 cm^{-1}, which was independent of t. The time course of these two absorption bands clearly indicates that the crystallization of PTHF occurs by ageing at 20°C. By further ageing, the network films became opaque, which prevented a quantitative absorption measurement.

The kinetics of isothermal crystallization of a bulk polymer from its melt is characterized by the Avrami equation. The fraction of the amorphous region that can crystallize is given by:

$$\ln(1 - X) = -kt^n \tag{5}$$

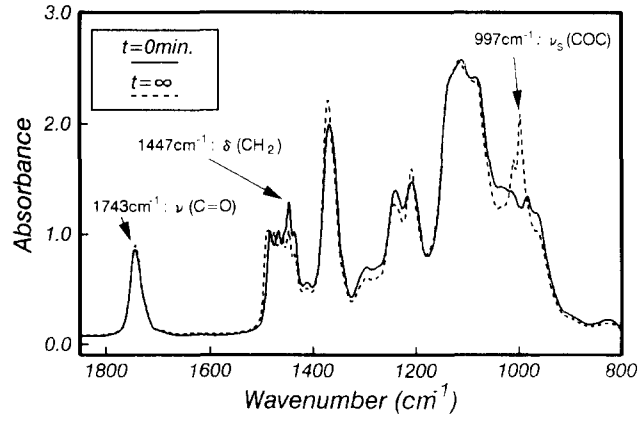

Figure 6 Infra-red absorption spectra for the end-linked PTHF networks of $t = 0$ (without ageing) and $t = \infty$ (aged at 20°C for 1 week)

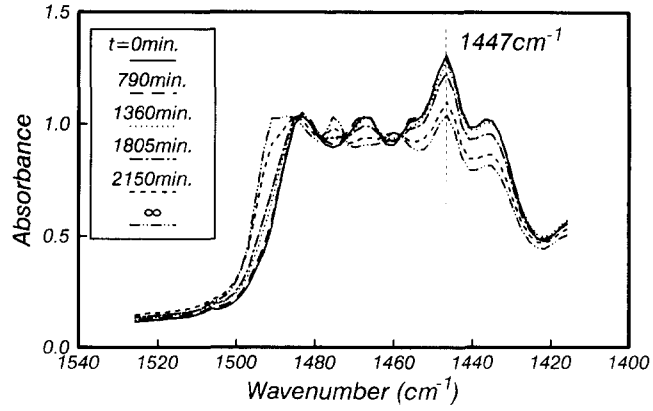

Figure 7 Time evolution of infra-red absorption spectra for the in-plane bending of CH_2, $\delta(CH_2)$, region

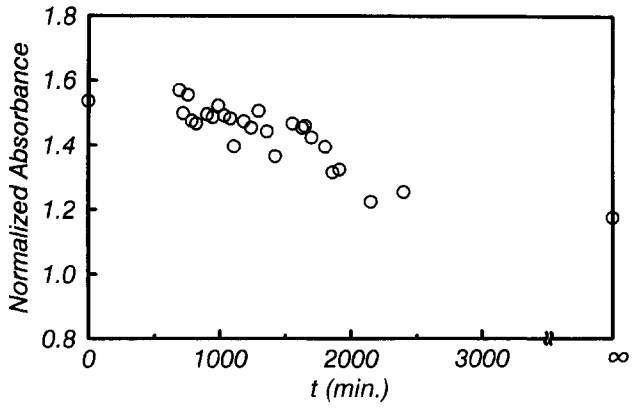

Figure 8 Ageing time dependence of the normalized absorbance at 1447 cm^{-1}

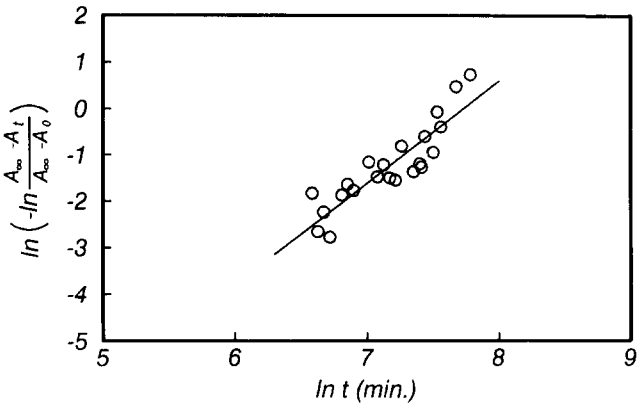

Figure 9 Avrami plot for the change of the absorbance with time

where X is the degree of crystallinity, and k and n are the Avrami constants. We apply this to the crystallization of the PTHF network. By assuming that the change of absorbance is proportional to X, the following relation is obtained:

$$\ln\left(-\ln\frac{A_\infty - A_t}{A_\infty - A_0}\right) = \ln k + n \ln t \qquad (6)$$

where A_i is the normalized absorbance for the film aged for $i = 0, t$, and ∞ (for 1 week). *Figure 9* shows the so-called Avrami plot. Although the data points are more or less scattered, these fall on a straight line with a slope of 2.2. Thus the Avrami exponent n is estimated to be 2.2 by i.r. analysis.

It should be noted that i.r. absorption analysis always involves uncertainty. In this study, we employed the peak height as the absorbance since the absorption band at 1447 cm^{-1} seemed to be similar in shape irrespective of the crystallization time. Caution was also paid by employing the internal standard, which was the band at 1743 cm^{-1}. However, we have to note that it is inevitable to allow some ambiguities in the reliability of the Avrami exponent. It should also be noted here that the irradiated part of the network film became partially clear when an opaque film was measured. This indicates that PTHF crystals are sensitive to i.r., which may result in an underestimation of the degree of crystallization by i.r.

D.s.c.

As shown in *Figures 3* and *8*, the crystallization of crosslinked PTHF is very slow and is in the order of days for the completion of the crystallization. Note that in the case of the corresponding PTHF prepolymer, the crystallization is complete in 30 min under the same conditions. Because of the slow crystallization kinetics, we could evaluate the degree of crystallization by d.s.c. measurements. As shown below, the heat of fusion of PTHF crystals is related to the degree of crystallization for PTHF networks aged for a given time. Recrystallization during a d.s.c. scan seems to be negligibly small in this particular case.

First of all, let us discuss the effect of the introduction of crosslinks to PTHF. *Figure 10* shows the comparison of d.s.c. thermograms for the prepolymer (dashed curve) and PTHF networks (solid curve). *Figure 10a* and *b* indicate that the samples have different thermal histories, such as as-prepared (*Figure 10a*) and aged at 20°C for 2 weeks after annealing at 60°C (*Figure 10b*). The d.s.c. measurement was carried out from −20 to +50°C. This means that the sample was quenched to −20°C before running a d.s.c. scan. *Figure 10c* shows the thermogram for the network aged for 1000 min. It has two endotherms, corresponding to those for the as-prepared (*Figure 10a*) and aged network (*Figure 10b*), respectively. This strongly indicates that the low-temperature endotherm is due to the melting of the crystals formed by rapid quenching to −20°C, whereas the high-temperature one is due to the melting of the crystals formed during the isothermal crystallization at 20°C. Note that such a double-peak endotherm was not observed in any of the prepolymer films having different ageing times. Since we will discuss this point later in relation to the analysis of the crystallization kinetics, we compare the two extreme cases, prepolymers *versus* network and as-prepared *versus* aged networks.

The melting temperature, T_m, and the heat of fusion, ΔH, of the prepolymer are higher and larger than those of the network, respectively. In case (a), T_m and ΔH are

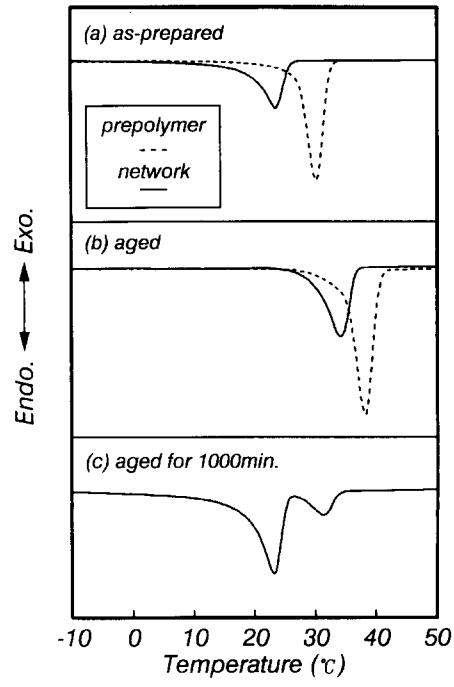

Figure 10 Comparison of the d.s.c. thermograms for the prepolymer (– – –) and the network (——). (a) Quenched to −20°C; (b) aged at 20°C for 2 weeks after annealing at 60°C; (c) aged network for 1000 min

30.2°C and 6.02 kJ mol^{-1} for the prepolymer and 23.6°C and 3.89 kJ mol^{-1} for the network. Those for case (b) are 38.1°C and 8.40 kJ mol^{-1} for the prepolymer and 34.3°C and 4.93 kJ mol^{-1} for the network. Note that the literature value of the enthalpy of fusion of 100% crystals of PTHF is 12.6 kJ mol^{-1} (ref. 15). In both cases, ΔH is smaller for the network than for the prepolymer, indicating that the degree of completion for the network is reduced by about 31% for case (a) and 39% for case (b). T_m for case (a) represents the melting endotherm of the crystals formed by the quenching process. These crystals are transformed to thicker crystals by ageing, which is case (b). The entropies of fusion for these samples are estimated to be 13.1 J mol^{-1} K^{-1} (quenched network) <16.0 J mol^{-1} K^{-1} (aged network) <19.9 J mol^{-1} K^{-1} (quenched prepolymer) <27.0 J mol^{-1} K^{-1} (aged prepolymer) <40.9 J mol^{-1} K^{-1} (pure PTHF crystals of $T_m=35$°C)[15], which indicate the order of completion of the PTHF crystals. Therefore it is clear that the degree of crystallization is significantly reduced by introducing crosslinks.

Since it became clear that the quenching process in a d.s.c measurement brings a tremendous effect on the crystallization even in polymers crystallized at such a slow rate, we discuss the quenching temperature dependence of the d.s.c. thermograms. *Figure 11* shows the d.s.c. thermograms of the as-prepared PTHF networks quenched to several temperatures. If the sample is quenched to -12°C or less, the d.s.c. thermogram has an endotherm at around 24°C. In the case of quenching to -1.4°C, a distinct crystallization exotherm was observed at 0°C. However, quenching to a temperature of 5°C and above did not show any endotherm. Thus it was found that the effect of quenching on the crystallization could be removed by changing the quenching temperature.

Figure 12 shows the ageing time dependence of d.s.c. thermograms for PTHF network films. The samples were quenched to 10°C and then d.s.c. thermograms were recorded by heating the sample at the rate of 5°C min^{-1}. As shown in the figure, the endotherm becomes large and the peak position shifts to the high-temperature side with ageing time t. Since this endotherm corresponds to the isothermal crystallization, we analysed the enthalpy of fusion, ΔH, as a function of t.

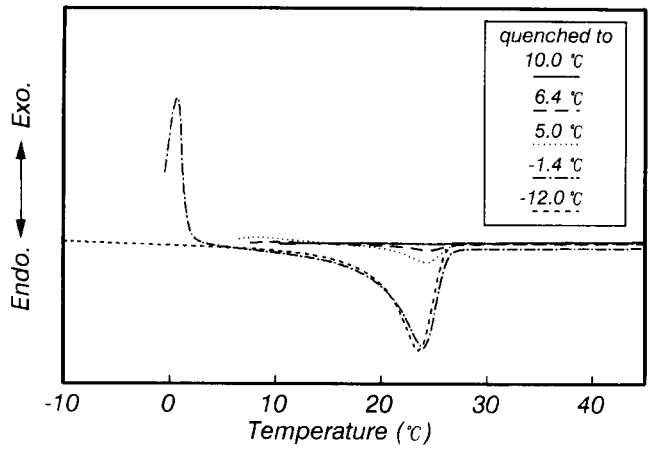

Figure 11 Quenching temperature dependence of d.s.c. thermograms for the end-linked PTHF networks

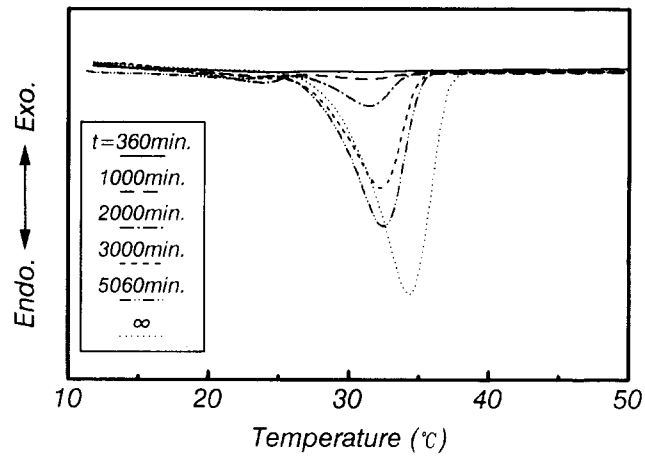

Figure 12 Variations of d.s.c. thermograms for the end-linked PTHF networks with the ageing time

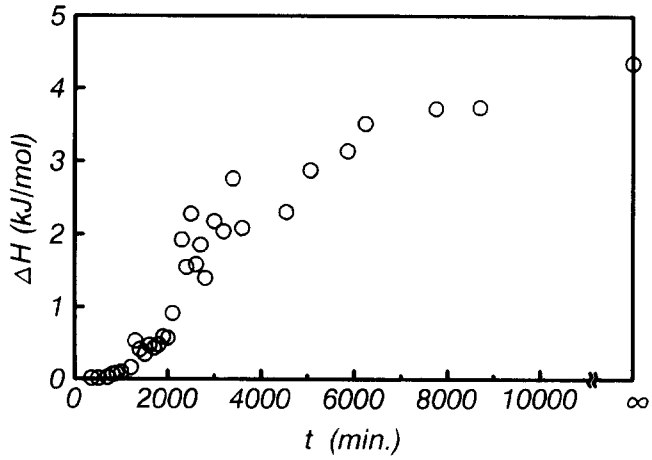

Figure 13 Ageing time dependence of the heat of fusion of PTHF crystals, ΔH

Figure 13 shows the time evolution of ΔH. ΔH is negligibly small until $t=1000$ min and then increases until 6000 min. This is a clear contrast to the result of the time course of M_c in *Figure 5*. M_c is very sensitive to the initiation of crystallization. The increasing rate of ΔH becomes slower for $t>6000$ min, which might be related to the secondary crystallization.

Similarly to the case of i.r. analysis, we assume that the change in ΔH is proportional to X. Then

$$\ln\left(-\ln\frac{\Delta H_\infty-\Delta H_t}{\Delta H_\infty}\right)=\ln k+n\ln t \qquad (7)$$

where ΔH_i denotes the enthalpy of fusion for the film aged for $i=0, t$ and ∞ (1 week). Data points fall on a straight line as shown in *Figure 14*. The slope gives the Avrami exponent, n, which is 2.4. This value is nearly equal to that obtained by the i.r. method. The obtained values of the Avrami exponent n being 2.2. and 2.4 may indicate that the PTHF crystals are formed via a homogeneous nucleation and are evolved three-dimensionally by diffusion control, the mechanism of which gives the theoretical value of $n=2.5$. This classification is based on a speculation that the crystallization must be greatly suppressed by the presence of crosslinks, resulting in diffusion control, and the crosslinks cannot be nuclei and are excluded from the crystallization (homogeneous

nucleation). However, further investigations are required to determine the crystallization kinetics of this type of polymer. We cite here a reference on PTHF crystallization by Trick and Ryan [16] for comparison. They obtained an Avrami exponent of 3 by dilatometry for PTHF linear polymers having a relatively high molecular weight, i.e. $M_n = 6700$.

Morphology of the PTHF network films

Figure 15 shows the evolution of the H_v-light scattering patterns of the PTHF networks during isothermal crystallization at 20°C and that of the prepolymer. P and A in the figure denote the directions of the polarizer and analyser, respectively. The appearance of a four-leaf clover pattern clearly indicates a formation of spherulites of PTHF and the spherulites grow with time.

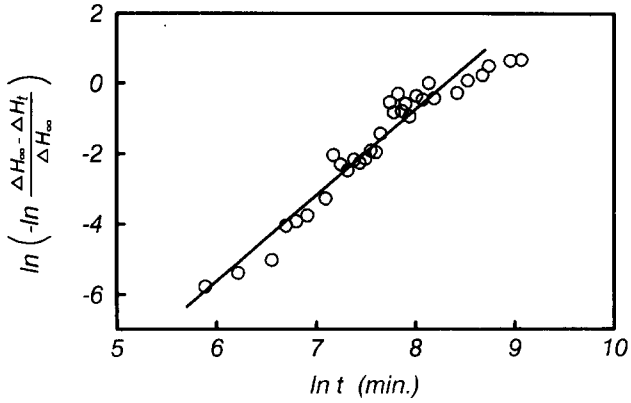

Figure 14 Avrami plot for the heat of fusion ΔH

Figure 16 shows polarized optical micrographs of the aged PTHF network and prepolymer films. In both films, well grown spherulites are observed. The sizes of the spherulites are estimated to be about 50 to 100 μm for the networks and 25 to 50 μm for the prepolymers. This figure clearly shows that a spherulitic superstructure is also formed for polymers having crosslinks although the rate of crystallization is greatly suppressed.

The appearance of the spherulitic textures in crystallization may support the proposed mechanism discussed above, i.e. the crystallization growth geometry being three-dimensional. Further analysis relating to the crystal morphology as well as crosslinking density dependence is now in progress.

CONCLUDING REMARKS

Telechelic PTHF with allyl end groups was synthesized and crosslinked with the tetrafunctional crosslinker. The crystallization kinetics of the PTHF network was investigated by measuring the mechanical and thermal properties and infra-red absorption spectroscopy. The mechanical behaviour gradually changed from that of

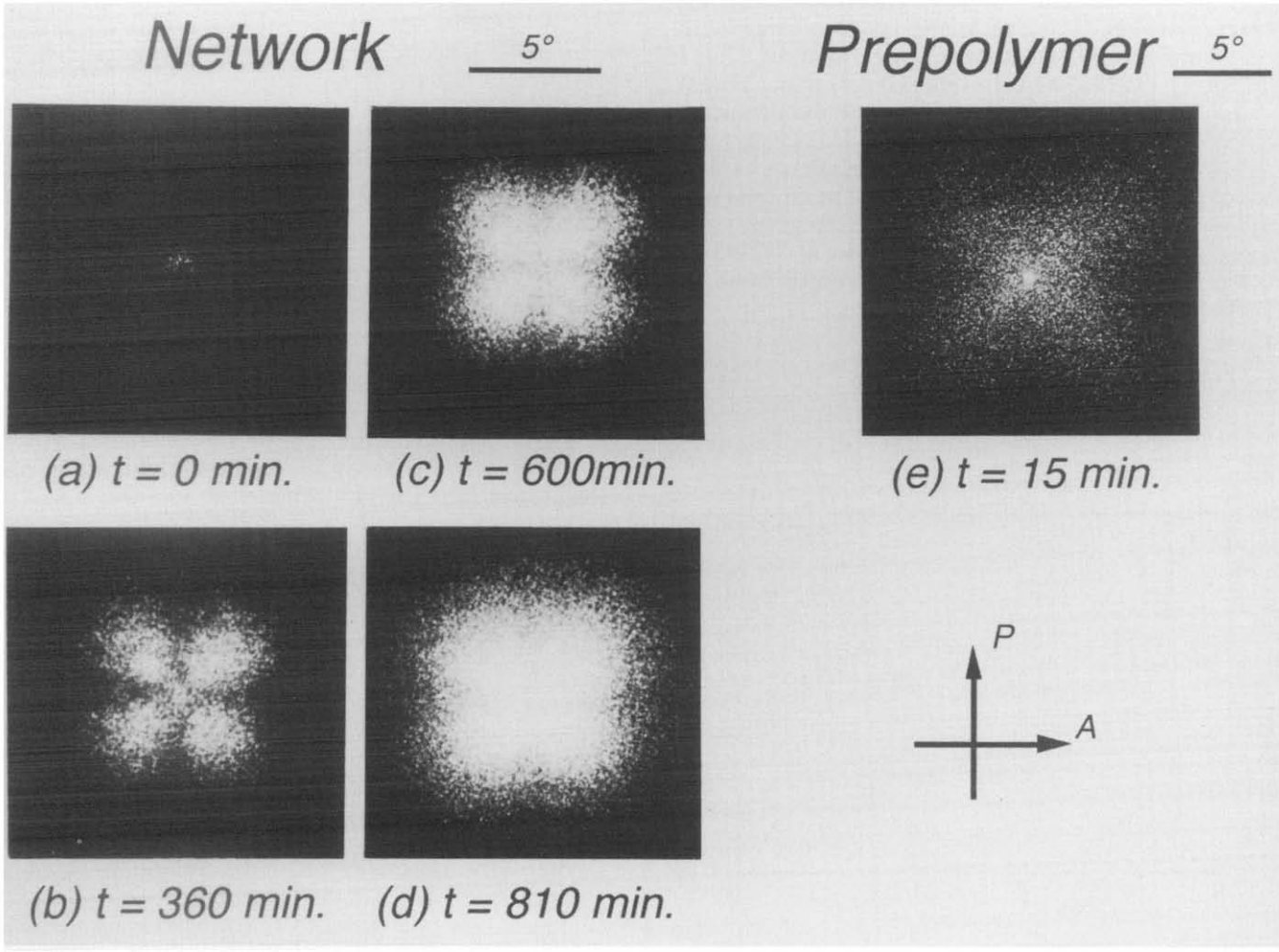

Figure 15 H_v-light scattering patterns for PTHF networks aged for $t =$ (a) 0, (b) 360, (c) 600 and (d) 810 min. (e) Prepolymer aged for 15 min. P and A indicate the directions of the polarizer and analyser, respectively

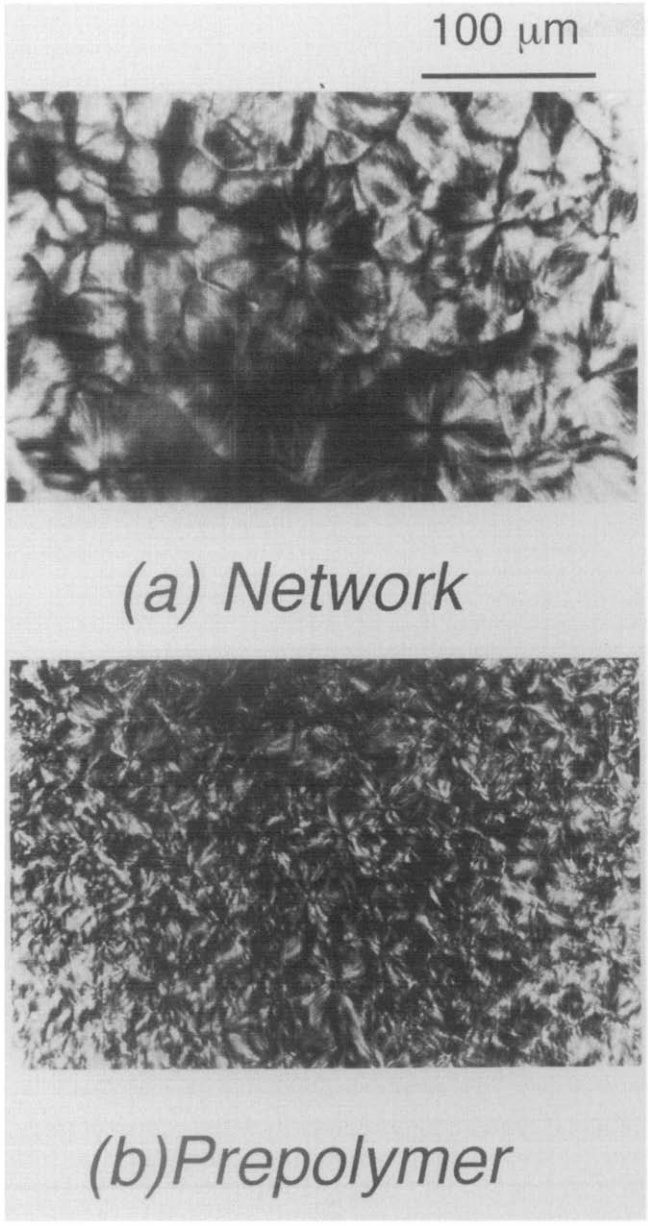

Figure 16 Polarized optical micrographs of (a) aged PTHF network and (b) prepolymer

typical elastomers to that of semicrystalline polymers in the process of the isothermal crystallization. The change of mechanical properties with ageing time was well interpreted by employing the Mooney–Rivlin equation as an increase in the apparent crosslinks of crystallites.

Quantitative analysis of the crystallization kinetics was carried out based on the i.r. and d.s.c. results. PTHF films quenched to −20°C exhibited two endotherms in d.s.c. during heating. The lower temperature endotherm is related to the rapid quenching of the film, while the higher is related to the isothermal crystallization. In the case of PTHF network film, the crystallization is greatly suppressed due to the presence of crosslinks. It takes the order of days to reach an equilibrium state for PTHF network film when crystallization occurs at room temperature. The Avrami constant, which characterized the primary crystallization, was found to be 2.2 and 2.4, by i.r. and d.s.c., respectively. The crystallization mechanism of the PTHF network is characterized by these values to be homogeneous nucleation, diffusion control and three-dimensional growth. It was also found that the secondary crystallization occurred very slowly after 6000 min. The formation of spherulitic superstructure was evidenced by light scattering and by optical microscopy.

ACKNOWLEDGEMENTS

The authors are indebted to Professor S. Kohjiya, Kyoto Institute of Technology, and to Dr T. Hashimoto, Fukui University, for valuable discussions and for the use of the laboratory facilities.

REFERENCES

1 Mark, J. E. *Adv. Polym. Sci.* 1982, **44**, 1
2 Flory, P. J. 'Principles of Polymer Chemistry', Cornell University Press, Ithaca, NY, 1953
3 James, H. M. and Guth, E. *J. Chem. Phys.* 1947, **15**, 669
4 Flory, P. J. *J. Chem. Phys.* 1977, **66**, 5720
5 Ball, R. C., Doi, M. and Edwards, S. F. *Polymer* 1981, **22**, 1010
6 Mark, J. E. and Sullivan, J. L. *J. Chem. Phys.* 1977, **66**, 1006
7 Llorente, M. A. and Mark, J. E. *J. Polym. Sci. Polym. Phys. Edn* 1980, **18**, 181
8 Andrady, A. L., Llorente, M. A. and Mark, J. E. *J. Chem. Phys.* 1980, **72**, 2282
9 Llorente, M. A., Andrady, A. L. and Mark, J. E. *J. Polym. Sci. Polym. Phys. Edn* 1981, **19**, 621
10 Jong, L. and Stein, R. S. *Macromolecules* 1991, **24**, 2323
11 Hanyu, A. and Stein, R. S. *Makromol. Chem. Macromol. Symp.* 1991, **45**, 189
12 Takahashi, H., Sakurai, S., Nakayama, M., Inui, Y., Shibayama, M., Hashimoto, T. and Nomura, S. *Kobunshi Ronbunshu* 1992, **49**, 907
13 Burdon, J., Farazmand, I., Stacey, M. and Tatlow, J. C. *J. Chem. Soc.* 1957, **1957**, 2574
14 Treloar, L. R. G. 'The Physics of Rubber Elasticity', 3rd Edn, Oxford University Press, Oxford, 1975
15 Brandrup, J. and Immergut, E. H. (Eds.) 'Polymer Handbook', 3rd Edn, Wiley, New York, 1989
16 Trick, G. S. and Ryan, J. M. *J. Polym. Sci., Part C* 1967, **18**, 93